Variational Gaussian Process Dynamical Systems

Anonymous Author(s)
Affiliation
Address
email

Abstract

High dimensional time series are endemic in applications of machine learning such as robotics (sensor data), computational biology (gene expression data), vision (video sequences) and graphics (motion capture data). Practical nonlinear probabilistic approaches to this data are required. In this paper we introduce the variational Gaussian process dynamical system. Our work builds on recent variational approximations for Gaussian process latent variable models to allow for simultaneous nonlinear dimensionality reduction, with automatic determination of data dimensionality, alongside learning a dynamical prior. We demonstrate our approach on a human motion capture data set and a series of high resolution video sequences.

1 Introduction

Nonlinear probabilistic modeling of high dimensional time series data is a key challenge for the machine learning community. A standard approach is to simultaneously apply a nonlinear dimensionality reduction to the data whilst governing the latent space with a nonlinear temporal prior. The key difficulty for such approaches is that analytic marginalization of the latent space is typically intractable. Markov chain Monte Carlo approaches can also be problematic as latent trajectories are strongly correlated making efficient sampling a challenge. One promising approach [[linking to the previous, is this implying a promising approach *to marginalisation of the latent space*? Because a few lines later we say "the latent variables are not marginalised (referring to MAP approaches)",maybe the reader will get confused?]] has been to extend the Gaussian process latent variable model [1, 2] with a dynamical prior for the latent space and seek a maximum a posteriori (MAP) solution for the latent points [3, 4, 5]. [6] further extend these models for fully Bayesian filtering in a robotics setting. We refer to this class of dynamical models based on the GP-LVM as Gaussian process dynamical systems (GPDS). However, the use of a MAP approximation for training these models presents key problems. Firstly, since the latent variables are not marginalised, the parameters of the dynamical prior cannot be optimized without the risk of overfitting. Further, the dimensionality of the latent space cannot be determined: adding further dimensions always increases the likelihood of the data. In this paper we build on recent developments in variational approximations for Gaussian processes [7, 8] to introduce a variational Gaussian process dynamical system (VGPDS) where latent variables are approximately marginalized through optimization of a rigorous lower bound on the marginal likelihood. As well as rigorously dealing with uncertainty in the latent space, this allows the parameters of the dynamical system to be determined and the dimensionality of the latent space [????] . The this?? approximation enables the application of our model to time series containing millions of dimensions and thousands of time points. We illustrate this by modeling human motion capture data and high dimensional video sequences.

2 The Model

Assume a multivariate times series dataset $\{\mathbf{y}_n, t_n\}_{n=1}^N$ where $\mathbf{y}_n \in \mathbb{R}^D$ is a data vector observed at time $t_n \in \mathbb{R}_+$. We are especially interested in cases where each $\mathbf{y}_n$ is a high dimensional vector and therefore we assume that there exists a low dimensional manifold that governs the generation of the data. Specifically, we assume a *temporal* latent function $\mathbf{x}(t) \in \mathbb{R}^Q$ (with $Q \ll D$), that comprises an intermediate *hidden* layer when generating the data, so that $\mathbf{y}_n$ is produced from $\mathbf{x}_n = \mathbf{x}(t_n)$ according to

$$y_{nd} = f_d(\mathbf{x}_n) + \epsilon_{nd}\,, \quad \epsilon_{nd} \sim \mathcal{N}(0, \beta^{-1}), \tag{1}$$

where $\mathbf{f}(\mathbf{x}) = [f_1(\mathbf{x}), \dots, f_D(\mathbf{x})]^\top$ is a latent mapping from the low dimensional space to the observation space and β is the inverse variance of the white Gaussian noise. We do not want to make strong assumptions about the functional form of the latent functions $(\mathbf{x}, \mathbf{f})$[1]. Instead we would like to infer them in a fully Bayesian non-parametric fashion using Gaussian processes [9]. Therefore, we assume that $\mathbf{x}$ is a multivariate Gaussian process indexed by time t and $\mathbf{f}$ is a different multivariate Gaussian process indexed by $\mathbf{x}$, and we write

$$x_q(t) \sim \mathcal{GP}(0, k_x(t_i, t_j)), \;\; q = 1, \dots, Q, \tag{2}$$

$$f_d(\mathbf{x}) \sim \mathcal{GP}(0, k_f(\mathbf{x}_i, \mathbf{x}_j)), \;\; d = 1, \dots, D. \tag{3}$$

Here, the individual components of the latent function $\mathbf{x}$ have taken to be independent sample paths drawn from a Gaussian process with kernel or covariance function [is ”kernel or covariance function” really needed in this form??] $k_x(t_i, t_j)$. Similarly, the components of $\mathbf{f}$ are independent draws from a Gaussian process with covariance function $k_f(\mathbf{x}_i, \mathbf{x}_j)$. These covariance functions, parametrized by parameters $\boldsymbol{\theta}_x$ and $\boldsymbol{\theta}_f$ respectively, play very distinct roles in the model. More precisely, k_x determines the properties of each temporal latent function $x_q(t)$. For instance, the use of an OU covariance function yields a Gauss-Markov autoregressive process for $x_q(t)$, while the squared-exponential kernel gives rise to very smooth and non-Markovian processes. The choice of a particular k_x is not expected to play a strictly determinative role for the overall performance of the method because the kernel's hyperparameters are optimised to fit the data in any case. However, certain kernels can fit better the characteristics of a given dataset. In our experiments, we focus on the squared exponential covariance function (RBF), the Matern $3/2$ which is only once differentiable and a periodic covariance function [9, 10] which can be used when data exhibit strong periodicity. These kernel functions take the form:

$$k_{x(rbf)}\left(t_i, t_j\right) = \sigma_{rbf}^2 e^{-\frac{(t_i - t_j)^2}{(2l_t^2)}}, \;\; k_{x(mat)}\left(t_i, t_j\right) = \sigma_{mat}^2 \left(1 + \frac{\sqrt{3}|t_i - t_j|}{l_t}\right) e^{\frac{-\sqrt{3}|t_i - t_j|}{l_t}},$$

$$k_{x(per)}\left(t_i, t_j\right) = \sigma_{per}^2 e^{-\frac{1}{2}\frac{sin^2\left(\frac{2\pi}{T}(t_i - t_j)\right)}{l_t}}. \tag{4}$$

On the other hand, the covariance function k_f determines the properties of the latent mapping $\mathbf{f}$ that maps each low dimensional variable $\mathbf{x}_n$ to the observed vector $\mathbf{y}_n$. We wish this mapping to be a non-linear but smooth function, and thus a suitable choice is the squared exponential kernel

$$k_f\left(\mathbf{x}_i, \mathbf{x}_j\right) = \sigma_{ard}^2 e^{-\frac{1}{2}\sum_{q=1}^Q w_q (x_{i,q} - x_{j,q})^2}, \tag{5}$$

which assumes a different scale w_q for each latent dimension. This, similarly to the variational Bayesian formulation of the GP-LVM [8], can enable an automatic relevance determination procedure, i.e. allowing Bayesian training to “switch off” unnecessary dimensions by driving the values of the corresponding scales to zero.

To summarize the above Bayesian non-parametric model, we can write down its finite joint probability density function induced by the finite observations. We introduce first some useful notation. The matrix $Y \in \mathbb{R}^{N \times D}$ will collectively denote all observed data so that its nth row corresponds to the data point $\mathbf{y}_n$. Similarly, the matrix $F \in \mathbb{R}^{N \times D}$ will denote the mapping latent variables, i.e. $f_{nd} = f_d(\mathbf{x}_n)$, associated with observations Y from (1). Analogously, $X \in \mathbb{R}^{N \times Q}$ will store all low dimensional latent variables $x_{nq} = x_q(t_n)$. Further, we will refer to columns of these matrices by the vectors $\mathbf{y}_d, \mathbf{f}_d, \mathbf{x}_q \in \mathbb{R}^N$. The joint probability density is written as

$$p(Y, F, X|\mathbf{t}) = p(Y|F)p(F|X)p(X|\mathbf{t}) = \prod_{d=1}^D p(\mathbf{y}_d|\mathbf{f}_d)p(\mathbf{f}_d|X) \prod_{q=1}^Q p(\mathbf{x}_q|\mathbf{t}), \tag{6}$$

[1]To simplify our notation, we often write $\mathbf{x}$ instead of $\mathbf{x}(t)$ and $\mathbf{f}$ instead of $\mathbf{f}(\mathbf{x})$. Later we also use a similar convention for the kernel functions by often writing them as k_f and k_x.

where $\mathbf{t} \in \mathbb{R}^N$ and $p(\mathbf{y}_d|\mathbf{f}_d)$ is a Gaussian likelihood function term defined from (1). Further, $p(\mathbf{f}_d|X)$ is a marginal GP prior such that

$$p(\mathbf{f}_d|X) = \mathcal{N}(\mathbf{f}_d|\mathbf{0}, K_{NN}), \tag{7}$$

where $K_{NN} = k_f(X, X)$ is the covariance matrix defined by the kernel function k_f and similarly $p(\mathbf{x}_q|\mathbf{t})$ is the marginal GP prior associated with the temporal function $x_q(t)$,

$$p(\mathbf{x}_q|\mathbf{t}) = \mathcal{N}\left(\mathbf{x}_q|\mathbf{0}, K_t\right), \tag{8}$$

where $K_t = k_x(\mathbf{t}, \mathbf{t})$ is the covariance matrix obtained by evaluating the kernel function k_x on the observed times $\mathbf{t}$.

Bayesian inference using the above model poses a huge computational challenge as, for instance, marginalization of the variables X that appear non-linearly inside the kernel matrix K_{NN} is troublesome. Practical approaches that have been considered until now (e.g. [5, 3]) marginalise out only F and seek a MAP solution for X. In the next section we describe how efficient variational approximations can be applied to marginalize X by extending the framework of [8].

2.1 Variational Bayesian training

The key difficulty with the Bayesian approach is propagating the prior density $p(X|\mathbf{t})$ through the nonlinear mapping. This mapping gives the expressive power to the model, but simultaneously renders the associated marginal likelihood,

$$p(Y|\mathbf{t}) = \int p(Y|F)p(F|X)p(X|\mathbf{t})\,\mathrm{d}X\,\mathrm{d}F, \tag{9}$$

intractable. We now invoke the variational Bayesian methodology to approximate the integral. Following a standard procedure [11], we introduce a variational distribution $q(\Theta)$ and compute the Jensen's lower bound $\mathcal{F}_v$ on the logarithm of (9),

$$\mathcal{F}_v(q, \boldsymbol{\theta}) = \int q(\Theta) \log \frac{p(Y|F)p(F|X)p(X|\mathbf{t})}{q(\Theta)}\,\mathrm{d}X\,\mathrm{d}F, \tag{10}$$

where $\boldsymbol{\theta}$ denotes the model's parameters. However, the above form of the lower bound is problematic becauce X (in the GP term $p(F|X)$) appears non-linearly inside the kernel matrix K_{NN} making the integration over X difficult. As shown in [8], this intractability is removed by applying the "data augmentation" principle. More precisely, we augment the joint probability model in (6) by including M extra samples of the GP latent mapping $\mathbf{f}$, known as inducing points, so that $\mathbf{u}_m \in \mathbb{R}^D$ is such a sample. The inducing points are evaluated at a set of pseudo-inputs $\tilde{X} \in \mathbb{R}^{M \times Q}$. The augmented joint probability density takes the form

$$p(Y, F, U, X, \tilde{X}|\mathbf{t}) = \prod_{d=1}^{D} p(\mathbf{y}_d|\mathbf{f}_d)p(\mathbf{f}_d|\mathbf{u}_d, X)p(\mathbf{u}_d|\tilde{X})p(X|\mathbf{t}), \tag{11}$$

where $p(\mathbf{u}_d|\tilde{X})$ is a zero-mean Gaussian with a covariance matrix K_{MM} constructed using the same function as for the GP prior (7). By dropping $\tilde{X}$ from our expressions, we write the augmented GP prior analytically (see [9]) as

$$p(\mathbf{f}_d|\mathbf{u}_d, X) = \mathcal{N}\left(\mathbf{f}_d|K_{NM}K_{MM}^{-1}\mathbf{u}_d, K_{NN} - K_{NM}K_{MM}^{-1}K_{MN}\right). \tag{12}$$

A key result in [8] is that a tractable lower bound (computed analogously to (10)) can be obtained by employing the following variational density:

$$q(\Theta) = q(F, U, X) = q(F|U, X)q(U)q(X) = \prod_{d=1}^{D} p(\mathbf{f}_d|\mathbf{u}_d, X)q(\mathbf{u}_d)q(X), \tag{13}$$

where $q(X) = \prod_{q=1}^{Q} \mathcal{N}\left(\mathbf{x}_q|\boldsymbol{\mu}_q, S_q\right)$ and $q(\mathbf{u}_m)$ is an arbitrary variational distribution. In [8] the next step is to assume independence in $q(X)$ (i.e. diagonal S_q). Here, in contrast, the posterior over the latent variables will have strong correlations, so S_q is taken to be a $N \times N$ full covariance matrix. Optimization of the variational lower bound provides an approximation to the true posterior

$p(X|Y)$. In the augmented probability model, the "difficult" term $p(F|X)$ appearing in (10) is now replaced with (12) and, eventually, it cancels out with the first factor of the variational distribution (13) so that F can now be marginalised out analytically. Given the above and after breaking the logarithm in (10), we obtain the final form of the lower bound (see supplementary material for more details)

$$\mathcal{F}_v(q, \boldsymbol{\theta}) = \hat{\mathcal{F}}_v - \text{KL}(q(X) \parallel p(X|\mathbf{t})), \tag{14}$$

with $\hat{\mathcal{F}}_v = \int q(X) \log p(Y|F) p(F|X) \, \mathrm{d}X \, \mathrm{d}F$. Both terms in (14) are now tractable. Note that the first of the above terms involves the data while the second one only involves the prior. All the information regarding datapoint correlations is captured in the KL term and the connection with the observations comes through the variational distribution. Therefore, the first term in (14) has the same analytical solution as the one derived in [8]. (14) can be maximized by using gradient-based methods[2]. However, when not factorizing $q(X)$ across data points yields $O(N^2)$ variational parameters to optimize. This issue is addressed in the next section.

2.2 Reparametrization and optimisation

The optimization involves the model parameters $\boldsymbol{\theta} = (\beta, \boldsymbol{\theta}_f, \boldsymbol{\theta}_t)$, the variational parameters $\{\boldsymbol{\mu}_q, S_q\}_{q=1}^Q$ from $q(X)$ and the inducing points,[3] $\tilde{X}$.

Optimization of the variational parameters appears challenging due to their large number and due to the correlations between them. However by reparametrizing $O\left(N^2\right)$ variational parameters according to the framework described in [12] we can obtain a set of $O(N)$ less correlated variational parameters. Specifically, we first take the derivatives of the variational bound (14) w.r.t S_q and $\boldsymbol{\mu}_q$ and set them to zero, in order to find the stationary points,

$$S_q = \left(K_t^{-1} + \Lambda_q\right)^{-1} \quad \textit{and} \quad \boldsymbol{\mu}_q = K_t \bar{\boldsymbol{\mu}}_q, \tag{15}$$

where $\Lambda_q = -2 \frac{\vartheta \hat{F}_v(q, \boldsymbol{\theta})}{\vartheta S_q}$ is a $N \times N$ diagonal, positive matrix and $\bar{\boldsymbol{\mu}}_q = \frac{\vartheta \hat{F}_v}{\vartheta \boldsymbol{\mu}_q}$ is a $N-$dimensional vector. The above stationary conditions tell us that, since S_q depends on a diagonal matrix Λ_q, we can reparametrize it using only the $N-$dimensional diagonal of that matrix, denoted by $\boldsymbol{\lambda}_q$. Then, we can optimise the $2(Q \times N)$ parameters $(\boldsymbol{\lambda}_q, \bar{\boldsymbol{\mu}}_q)$ and obtain the original parameters using (15).

2.3 Learning from multiple sequences

Our objective is to model multivariate time series. A given data set may consist of a group of independently observed sequences, each with a different length (e.g. in human motion capture data several walks from a subject). We would like our model to capture the underlying commonality of these data. We handle this by associating each sequence s with a different subspace $X^{(s)}$ of a shared latent manifold; the mappings $\mathbf{f}$ and the model parameters are shared for all sequences [KEEP THIS??]. More specifically, if $Y = \left[Y^{(1)}, ..., Y^{(S)}\right]^\top$ is a concatenation of S blocks (sequences), then each one is assumed to be generated by $Y^s = \mathbf{f}(X^{(s)})$ plus some noise and then the likelihood is written in the form,

$$p\left(Y^{(1)}, ..., Y^{(S)} | \mathbf{f}\right) p\left(\mathbf{f} | X^{(1)}, ..., X^{(S)}\right) \tag{16}$$

To account only for time correlations within the same sequence we force the time covariance matrix K_t to be block-diagonal with each block capturing the dependencies implied by the datapoints of a single sequence.

3 Predictions

Our algorithm models the temporal evolution of a dynamical system. It should be capable of generating completely new sequences or reconstructing missing observations from partially observed data. For generating novel sequence given training data the model requires a time vector $\mathbf{t}_*$ as input

[2] See supplementary material for more detailed derivation of (14) and for the equations for the gradients.

[3] We will use the term "variational parameters" to refer only to the parameters of $q(X)$ although the inducing points are also variational parameters.

and computes a density $p(Y_*|Y, \mathbf{t}, \mathbf{t}_*)$. For reconstruction of partially observed data the timestamp information is additionally accompanied by a partially observed sequence $Y_*^p \in \mathbb{R}^{N_* \times D_p}$ from the whole $Y_* = (Y_*^p, Y_*^m)$, where p and m are set of indices indicating the present (i.e. observed) and missing dimensions of Y_* respectively, so that $p \cup m = \{1, \ldots, D\}$. We reconstruct the missing dimensions by computing the Bayesian predictive distribution $p(Y_*^m|Y_*^p, Y, \mathbf{t}_*, \mathbf{t})$. The predictive densities can also be used as estimators for tasks like generative Bayesian classification. For optimal performance test data is presented jointly to model the correlations in the augmented set $[Y, Y_*]^\top$ correctly. Whilst time stamp information is always provided, in the next section we drop its dependence to avoid notational clutter.

3.1 Totally unobserved data

To approximate the predictive density, we will need to introduce the underlying latent function values $F_* \in \mathbb{R}^{N_* \times D}$ (the noisy-free version of Y_*) and the latent variables $X_* \in \mathbb{R}^{N_* \times Q}$. We write the predictive density as

$$p(Y_*|Y) = \int p(Y_*, F_*, X_*|Y_*, Y)dF_*dX_* = \int p(Y_*|F_*)p(F_*|X_*, Y)p(X_*|Y)dF_*dX_*. \quad (17)$$

The term $p(F_*|X_*, Y)$ is approximated according by

$$q(F_*|X_*) = \int \prod_{d \in D} p(\mathbf{f}_{*,d}|\mathbf{u}_d, X_*)q(\mathbf{u}_d)d\mathbf{u}_d = \prod_{d \in D} q(\mathbf{f}_{*,d}|X_*), \quad (18)$$

where $q(\mathbf{f}_{*,d}|X_*)$ is a Gaussian that can be computed analytically.The term $p(X_*|Y)$ in eq. (17) is approximated by a Gaussian variational distribution $q(X_*)$,

$$p(X_*|Y) \approx \int p(X_*|X)q(X)dX = \langle p(X_*|X) \rangle_{q(X)} = q(X_*) = \prod_{q=1}^{Q} q(\mathbf{x}_{*,q}), \quad (19)$$

where $p(X_{*,q}|X)$ can be found from the conditional GP prior (see [9]). We can then write

$$\mathbf{x}_{*,q} = \boldsymbol{\alpha} \mathbf{x}_q + \boldsymbol{\epsilon}, \quad (20)$$

where $\boldsymbol{\alpha} = K_{*N}K_t^{-1}$ and $\boldsymbol{\epsilon} \sim \mathcal{N}\left(\mathbf{0}, K_{**} - K_{*NK_t^{-1}K_{N*}}\right)$. Also, $K_t = k_t(\mathbf{t}, \mathbf{t})$, $K_{*N} = k_t(\mathbf{t}_*, \mathbf{t})$ and $K_{**} = k_t(\mathbf{t}_*\mathbf{t}_*)$. Given the above, we know a priori that (19) is a Gaussian and by taking expectations over $q(X)$ in the r.h.s. of (20) we find the mean and covariance of $q(X_*)$. Substituting for the equivalent forms of $\boldsymbol{\mu}_q$ and S_q from section 2.2 we obtain the final solution

$$\mu_{x_{*,q}} = \mathbf{k}_{*N}\bar{\mu}_q \quad (21)$$

$$\text{var}(x_{*,q}) = k_{**} - \mathbf{k}_{*N}(K_t + \Lambda_q^{-1})^{-1}\mathbf{k}_{N*}. \quad (22)$$

(17) can then be written as:

$$p(Y_*|Y) = \int p(Y_*|F_*)q(F_*|X_*)q(X_*)dF_*dX_* = \int p(Y_*|F_*) \langle q(F_*|X_*) \rangle_{q(X_*)} dF_* \quad (23)$$

Although the expectation appearing in the above integral is not a Gaussian, its moments can be found analytically [9, 13],

$$\mathbb{E}(F_*) = B^\top \Psi_1^* \quad (24)$$

$$\text{Cov}(F_*) = B^\top \left(\Psi_2^* - \Psi_1^*(\Psi_1^*)\top\right) B + \Psi_0^* I - \text{Tr}\left[\left(K_{MM}^{-1} - (K_{MM} + \beta\Psi_2)^{-1}\right)\Psi_2^*\right] I, \quad (25)$$

where $B = \beta \left(K_{MM} + \beta\Psi_2\right)^{-1} \Psi_1^\top Y$, $\Psi_0^* = \langle k_f(X_*, X_*) \rangle$, $\Psi_1^* = \langle K_{M*} \rangle$ and $\Psi_2^* = \langle K_{M*}K_{*M} \rangle$. All expectations are taken w.r.t. $q(X_*)$ and can be calculated analytically, while K_{M*} denotes the cross-covariance matrix between the training inducing inputs Z and X_*. Finally, since Y_* is just a noisy version of F_*, the mean and covariance of (23) is just computed as: $\mathbb{E}(Y_*) = \mathbb{E}(F_*)$ and $\text{Cov}(Y_*) = \text{Cov}(F_*) + \beta^{-1}I_{N_*}$.

3.2 Partially observed test data

The expression for the predictive density $p(Y_*^m|Y_*^p, Y)$ follows exactly as in section 3.1 but we need to compute probabilities for Y_*^m instead of Y_* and Y is replaced with (Y, Y_*^p) in all conditioning sets. Similarly, F is replaced with F^m. Now $q(X_*)$ cannot be found analytically as in eq. 3.1; instead, it is optimised so that Y_*^p are taken into account. This is done by maximising the variational lower bound on the marginal likelihood:

$$\begin{aligned} p(Y_*^p, Y) &= \int p(Y_*^p, Y|X_*, X)p(X_*, X)\mathrm{d}X_*\mathrm{d}X \\ &= \int p(Y^m|X)p(Y_*^p, Y^p|X_*, X)p(X_*, X)\mathrm{d}X_*\mathrm{d}X, \end{aligned}$$

Assuming a variational distribution $q(X_*, X)$ and using Jensen's inequality we obtain the lower bound

$$\begin{aligned} &\int q(X_*, X)\log\frac{p(Y^m|X)p(Y_*^p, Y^p|X_*, X)p(X_*, X)}{q(X_*, X)}\mathrm{d}X_*\mathrm{d}X \\ =& \int q(X)\log p(Y^m|X)\mathrm{d}X + \int q(X_*, X)\log p(Y_*^p, Y^p|X_*, X)\mathrm{d}X_*\mathrm{d}X \\ -& \operatorname{KL}[q(X_*, X)||p(X_*, X)] \end{aligned} \tag{26}$$

This quantity can now be maximized in the same manner as for the bound of the training phase. Unfortunately, this means that the variational parameters that are already optimised from the training procedure cannot be used here because X and X_* are coupled in $q(X_*, X)$. A much faster but less accurate method would be to decouple the test from the training latent variables by imposing the factorisation $q(X_*, X) = q(X)q(X_*)$. Then, equation (26) would break into terms containing X, X_* or both. The ones containing only X could then be treated as constants.

4 Handling Very High Dimensional Datasets

Given that our training framework is built on a sparse approach, the approximation is tractable for relatively large datasets (thousands of time points, N). However ["however"? Isn't it like contrasting a positive fact with another positive fact??], the model scales only linearly with the number of dimensions D. Specifically, the number of dimensions only matters when performing calculations involving the data matrix Y. In the final form of the lower bound (and consequently in all of the derived quantities, such as gradients) this matrix only appears in the form $YY^\top$ which can be precomputed. This means that when $N \ll D$, we can calculate $YY^\top$ only once and then substitute Y with the SVD (or Cholesky decomposition) of $YY^\top$. In this way, we can work with an $N \times N$ instead of an $N \times D$ matrix. Practically speaking, this allows us to work with data sets involving millions of features. In our experiments we model directly the pixels of HD quality video, exploiting this trick.

5 Experiments

We consider two different types of high dimensional time series [the mocap is 59-dim, is that considered to be high dim?], a human motion capture data set consisting of different walks and high resolution video sequences. The experiments are intended to explore the various properties of the model and to evaluate its performance in different tasks (prediction, reconstruction, generation of data). More figures and examples are included in the supplementary material.

5.1 Motion capture data

We followed [14, 15] in considering motion capture data of walks and runs taken from subject 35 in the CMU motion capture database. We treated each motion as an independent sequence. The data set was constructed and preprocessed as described in [15]. This results in 2613 59-dimensional frames split into 31 training sequences with an average length of 84 frames each.

The model is jointly trained, as explained in section 2.3, on both walks and runs, challenging the algorithm to learn a common latent space for these motions. At test time we investigate the ability of the model to reconstruct test data from a previously unseen sequence given partial information for the test targets. This is tested once by providing only the dimensions which correspond to the body of the subject and once by providing those that correspond to the legs.

We compare with results in [15], which used MAP approximations for the dynamical models, and against nearest neighbour. We can also indirectly compare with the binary latent variable model (BLV) of [14] which used a slightly different data preprocessing. We assess the performance using the cumulative error per joint in the scaled space defined in [14] and by the root mean square error in the angle space suggested by [15]. Our model was initialized with nine latent dimensions. We performed two runs, once using the Matern covariance function for the dynamical prior and once using the RBF. From table 1 we see the variational Gaussian process dynamical system considerably outperforms the other approaches. The appropriate latent space dimensionality for the data was automatically inferred by our models, since the one using the RBF kernel retained four dimensions whereas the model using the Matern kept only three. The other latent dimensions were completely switched off by the ARD parameters. The best performance for the legs and the body reconstruction was achieved by the VGPDS model that used the Matern and the RBF covariance function respectively.

Table 1: Errors obtained for the motion capture dataset considering nearest neighbour in the angle space (NN) and in the scaled space(NN sc.), GPLVM, BLV and VGPDS. CL / CB are the leg and body datasets as preprocessed in [14], L and B the corresponding datasets from [15]. SC corresponds to the error in the scaled space, as in Taylor et al. while RA is the error in the angle space. The best error per column is in bold.

Data	CL	CB	L	L	B	B
Error Type	SC	SC	SC	RA	SC	RA
BLV	11.7	**8.8**	-	-	-	-
NN sc.	22.2	**20.5**	-	-	-	-
GPLVM (Q = 3)	-	-	11.4	3.40	16.9	2.49
GPLVM (Q = 4)	-	-	9.7	3.38	20.7	2.72
GPLVM (Q = 5)	-	-	13.4	4.25	23.4	2.78
NN sc.	-	-	13.5	4.44	20.8	2.62
NN	-	-	14.0	4.11	30.9	3.20
VGPDS (RBF)	-	-	8.19	3.57	**10.73**	**1.90**
VGPDS (Matern 3/2)	-	-	**6.99**	**2.88**	14.22	2.23

5.2 High dimensional video sequences

For our second set of experiments we considered video sequences. Such sequences are typically preprocessed before modelling to extract informative features and reduce the dimensionality of the problem. Here we work directly with the raw pixel values to demonstrate the ability of the VGPDS to model data with a vast number of features. This also allows us to directly sample video from the learned model.

Need a bit more detail here (also mention that only ocean is HD) Firstly we used the model to reconstruct partially observed frames from video test sequences. The mean squared error per pixel was measured to compare with the $k-$Nearest Neighbour (NN) method, for $k \in (1, .., 5)$ (we only present the error achieved for the best k per case). The datasets considered are the following: firstly, the 'Missa' dataset[4], a standard benchmark used in image processing. This 103,680-dimensional video, showing a woman talking for 150 frames, is quite challenging as there are translations in the pixel space. We also considered a HD video of dimensionality 9×10^5 that shows an artificially created scene of ocean waves as well as a $?-$dimensional video[5] showing a dog running for 60 frames. The later is a dataset periodic in nature but only approximately, as it is a real-world video (otherwise the NN method would achieve perfect reconstruction). For the first two videos we used the

[4]www.cipr.rpi.edu

[5]available at: ...

Matern and RBF kernels respectively to model the dynamics and interpolated to reconstruct blocks of frames chosen from the whole sequence. For the the 'dog' dataset we constructed a compound kernel $k_t = k_{t(rbf)} + k_{t(periodic)}$, where the RBF term is employed to capture the divergence from the approximately periodic pattern. We then used our model to reconstruct the last 7 frames, thus performing extrapolation. As can be seen in table 2, our method outperformed NN in all cases. The results are also demonstrated visually in figure 1 and in the supplementary material.

Table 2: The mean squared error per pixel for VGPDS and NN for the three datasets (measured only in the missing inputs). The number of latent dimensions selected by our model is in parenthesis.

	Missa	Ocean	Dog
VGPDS	3.12 ($Q = ...$)	9.36 ($Q = 9$)	4.01 ($Q = 6$)
NN	3.26	9.53	4.15

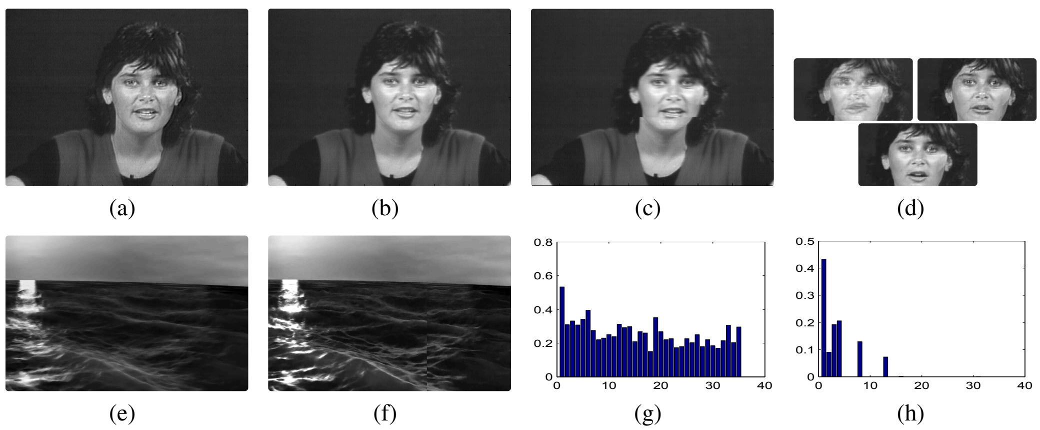

Figure 1: 1(a) and 1(c) demonstrate the reconstruction achieved by VGPDS and NN respectively for the original frame 1(b) taken from the 'missa' video. Another example (cropped to fit) can be seen in 1(d) I will add tags to each image to show the method. 1(e) (VGPDS) and 1(f) (NN) depict the reconstruction achieved for a frame of the 'ocean' dataset. Finally, we demonstrate the ability of the model to automatically select the latent dimensionality by showing the initial lengthscales (fig: 1(g)) of the ARD kernel and the values taken after training (fig: 1(h)) on the 'dog' dataset.

As a second task, we used our generative model to create new samples and effectively generate a new video sequence. This is possible when the training examples are at least approximately periodic in nature. The model was trained on 60 frames (time-stamps $[t_1, t_{60}]$) of the aforementioned 'dog' video and generated the frames which correspond to the next 40 time points in the future. The only input given for the test phase was, thus, the test time vector $[t_{61}, t_{100}]$. The challenge is not only to generate a non-blurry video, but also to resume the motion while performing the transition from the training to the test frames. Indeed, the frame in t_{61} is smoothly following the one in t_{60} and the overall result achieved is quite realistic, as can be seen in figure 2.

6 Discussion and future work

We have introduced a fully Bayesian approach for modelling dynamical systems through probabilistic nonlinear dimensionality reduction. Marginalizing the latent space and reconstructing data using Gaussian processes results in a very generic model for capturing complex, non-linear correlations even in very high dimensional data, without having to perform any data preprocessing or exhaustive search for defining the model's structure and parameters.

Our method's effectiveness has been demonstrated in two tasks; firstly, in modelling human motion capture data and, secondly, in reconstructing and generating raw, very high dimensional video sequences. A promising future direction to follow would be to enhance our formulation with domain-specific knowledge encoded, for example, in more sophisticated covariance functions or in the way

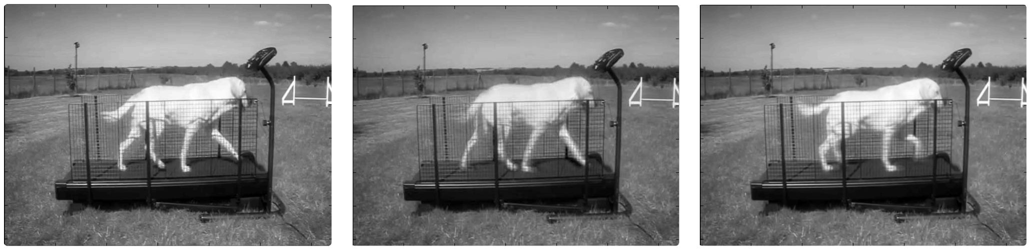

(a) (b) (c)

Figure 2: The last frame of the training video 2(a) is smoothly followed by the first frame 2(b) of the generated video. A subsequent generated frame can be seen in 2(c).

that data are being preprocessed. Thus, we can obtain application-oriented methods to be used for tasks in areas such as vision and finance.

References

[1] N. Lawrence, "Probabilistic non-linear principal component analysis with Gaussian process latent variable models," *Journal of Machine Learning Research*, vol. 6, pp. 1783–1816, 2005.

[2] N. D. Lawrence, "Gaussian process latent variable models for visualisation of high dimensional data," in *In NIPS*, p. 2004, 2004.

[3] J. M. Wang, D. J. Fleet, and A. Hertzmann, "Gaussian process dynamical models," in *In NIPS*, pp. 1441–1448, MIT Press, 2006.

[4] J. M. Wang, D. J. Fleet, and A. Hertzmann, "Gaussian process dynamical models for human motion," vol. 30, no. 2, pp. 283–298, 2008.

[5] N. D. Lawrence, "Hierarchical Gaussian process latent variable models," in *In International Conference in Machine Learning*, 2007.

[6] J. Ko and D. Fox, "GP-BayesFilters: Bayesian filtering using Gaussian process prediction and observation models," *Auton. Robots*, vol. 27, pp. 75–90, July 2009.

[7] M. Titsias, "Variational learning of inducing variables in sparse Gaussian processes," *Journal of Machine Learning Research - Proceedings Track*, vol. 5, pp. 567–574, 2009.

[8] M. Titsias and N. D. Lawrence, "Bayesian Gaussian process latent variable model," *Journal of Machine Learning Research - Proceedings Track*, vol. 9, pp. 844–851, 2010.

[9] C. E. Rasmussen and C. Williams, *Gaussian Processes for Machine Learning*. MIT Press, 2006.

[10] D. J. C. MacKay, "Introduction to Gaussian processes," in *Neural Networks and Machine Learning* (C. M. Bishop, ed.), NATO ASI Series, pp. 133–166, Kluwer Academic Press, 1998.

[11] C. M. Bishop, *Pattern Recognition and Machine Learning (Information Science and Statistics)*. Springer, 1st ed. 2006. corr. 2nd printing ed., Oct. 2007.

[12] M. Opper and C. Archambeau, "The variational Gaussian approximation revisited," *Neural Computation*, vol. 21, no. 3, pp. 786–792, 2009.

[13] A. Girard, C. E. Rasmussen, J. Quiñonero-Candela, and R. Murray-Smith, "Gaussian process priors with uncertain inputs - application to multiple-step ahead time series forecasting," in *Neural Information Processing Systems*, 2003.

[14] G. W. Taylor, G. E. Hinton, and S. Roweis, "Modeling human motion using binary latent variables," in *Advances in Neural Information Processing Systems*, p. 2007, MIT Press, 2006.

[15] N. D. Lawrence, "Learning for larger datasets with the Gaussian process latent variable model," *Journal of Machine Learning Research - Proceedings Track*, vol. 2, pp. 243–250, 2007.